

# **Measurements of Reactive Nitrogen in the Stratosphere**

B. Sen, G.C. Toon, G. El. Osterman, J.-F. Blavier, J.J. Margitan, and R.J. Salawitch  
Jet Propulsion Laboratory, California Institute of Technology, Pasadena, California

G.K. Yue  
NASA Langley Research Center, Hampton, VA

Edit Date: 24.3.1997

Proposed Journal: Journal of Geophysics] Research

Received \_\_\_\_\_ ; accepted \_\_\_\_\_

Short title: STRATOSPHERIC NO<sub>x</sub> OBSERVATIONS

## **Abstract.**

We present volume mixing ratio profiles of NO, NO<sub>2</sub>, HNO<sub>3</sub>, HNO<sub>4</sub>, N<sub>2</sub>O<sub>5</sub>, and ClNO<sub>3</sub> and their composite budget (NO<sub>y</sub>), from 20 to 39 km, measured remotely in solar occultation by the JPL MkIV Interferometer during a high-altitude balloon flight from Fort Sumner, New Mexico (35°N) on 25 September 1993. In general, observed profiles agree well with values calculated using a photochemical steady state model constrained by simultaneous MkIV observations of long-lived precursors and aerosol surface area from SAGE II. The measured variation of concentrations of NO<sub>x</sub> (= NO + NO<sub>2</sub>) and N<sub>2</sub>O<sub>5</sub> between sunrise and sunset reveals the expected ≈2:1 stoichiometry at all altitudes. Despite relatively good agreement between theory and observation for profiles of NO and HNO<sub>3</sub>, the observed concentration of NO<sub>2</sub> becomes progressively higher than model values below 30 km, with the discrepancy reaching 33% at 22 km. Consequently, the observations suggest an incomplete understanding of factors that regulate the NO/NO<sub>2</sub> and NO<sub>2</sub>/HNO<sub>3</sub> ratios below 30 km.

Data collected during September 1993 and flights in September 1990 and April 1993 at 35°N reveal a decrease in the NO<sub>x</sub>/NO<sub>y</sub> ratio for increasing aerosol surface area, following the eruption of Mt. Pinatubo. These observations are consistent with the heterogeneous hydrolysis of N<sub>2</sub>O<sub>5</sub> being the dominant sink of NO<sub>x</sub> between altitudes of 18 and 24 km for the encountered conditions (e.g., surface area as high as 14  $\mu\text{m}^2\text{cm}^{-3}$ , and temperature from 209 to 219 K).

## Introduction

Reactions involving NO and NO<sub>2</sub> constitute the primary process for chemical removal of stratospheric O<sub>3</sub> between altitudes of approximately 24 to 36 km [e.g., Crutzen, 1970; Johnston, 1971]. The abundance of NO, (= NO + NO<sub>2</sub>) regulates the concentration of chlorine monoxide (ClO) as well as the ratio of OH to HO<sub>2</sub> in the mid-latitude lower stratosphere for air unaffected by polar stratospheric clouds [e.g., Wennberg et al., 1994]. The partitioning of NO<sub>x</sub> relative to N<sub>2</sub>O<sub>5</sub> and HNO<sub>3</sub>, the dominant reservoirs of the nitrogen oxide family of gases (NO<sub>y</sub>, defined as the sum of the concentration of NO<sub>x</sub>, HNO<sub>3</sub>, HNO<sub>4</sub>, 2·N<sub>2</sub>O<sub>5</sub>, ClNO<sub>3</sub>, BrNO<sub>3</sub>, NO<sub>3</sub>, and HNO<sub>2</sub>), is controlled by a variety of processes, including some occurring on the surface of sulfate aerosols [e.g., McElroy et al., 1992].

Increased aerosol loading following the eruption of Mt. Pinatubo in June 1991 led to reduced levels of NO<sub>x</sub>, increased concentrations of ClO, and accelerated photochemical removal of O<sub>3</sub> near 20 km consistent with the heterogeneous reaction of N<sub>2</sub>O<sub>5</sub> + H<sub>2</sub>O being the dominant sink for NO<sub>x</sub> [e.g., Fahay et al., 1993; Kawa et al., 1993; Salawitch et al., 1994a,b; Stimpfle et al., 1994]. ~alloon-borne? *in situ* observations of NO, NO<sub>y</sub>, O<sub>3</sub>, and aerosol surface area [Kondo et al., 1997]; NO<sub>2</sub> and HNO<sub>3</sub> [Webster et al., 1994]; and ClO, NO, and O<sub>3</sub> [Dessler et al., 1993] each show a reduction in NO/NO<sub>y</sub> for increased aerosol loading consistent also with chemistry driven largely by the heterogeneous hydrolysis of N<sub>2</sub>O<sub>5</sub>. However, ground based observations of the decrease in the column abundance of NO<sub>2</sub> and simultaneous increase in column HNO<sub>3</sub> following the eruption of Mt. Pinatubo indicate the need for additional heterogeneous sinks of NO<sub>x</sub> to quantitatively account for the measured decrease in NO<sub>2</sub>/HNO<sub>3</sub> [Koike et al., 1994]. *In situ* observations of NO, NO<sub>2</sub>, ClO, and O<sub>3</sub> at mid-latitudes during the spring of 1993 have revealed a troubling discrepancy in our understanding the NO/NO<sub>2</sub> ratio near 20 km [Jaeglé et al., 1994], although more recent observations over a wider range of latitudes reveal good agreement between theory and observation of this ratio as well

as the  $\text{NO}_x/\text{NO}_y$  ratio [Gao *et al.*, 1997]. Finally, an analysis of *in situ* observations of HCl obtained from 1991 to 1996 suggests heterogeneous reactions other than  $\text{N}_2\text{O}_5 + \text{H}_2\text{O}$  exert a dominant influence on the composition of the mid-latitude stratosphere [Webster *et al.*, 1997].

The JPL MarkIV Interferometer (MkIV) balloon observations reported here represent the first simultaneous measurements of profiles for all major  $\text{NO}_y$  species in the same airmass along with the important precursors (e.g.,  $\text{O}_3$ ,  $\text{CH}_4$ ,  $\text{H}_2\text{O}$ ,  $\text{C}_2\text{H}_6$ ,  $\text{HCl}$ ,  $\text{CO}$ ) that allow a stringent comparison to calculated profiles. Furthermore, noon, sunset, and sunrise profiles of  $\text{NO}_x$  and  $\text{N}_2\text{O}_5$  were measured in the same airmass, allowing their diurnal behavior to be examined. Previous studies of diurnal behavior have either only obtained measurements over a limited altitude range [Webster *et al.*, 1990; Kondo *et al.*, 1990], have not measured all the relevant species [Roscoe *et al.*, 1990; Chance *et al.*, 1996], or have not measured them all simultaneously in the same air mass [Russell *et al.*, 1988; Rinsland *et al.*, 1996].

Our analyses of the MkIV observations test our understanding of processes that regulate (a)  $\text{NO}_x$ , the component of the  $\text{NO}_y$  that reacts directly with  $\text{O}_3$ , (b)  $\text{HNO}_3$ , the dominant  $\text{NO}_y$  species at low altitudes, (c)  $\text{N}_2\text{O}_5$ , the component that links reactive and reservoir  $\text{NO}_y$ , (d)  $\text{HN}_3$ , a minor reservoir that tests our understanding of  $\text{HO}_x$  ( $= \text{OH} + \text{HO}_2$ ), and (e)  $\text{ClNO}_3$ , the species that couples reactive nitrogen and chlorine. Additionally, our study focuses on testing our understanding of the processes that regulate the concentration of  $\text{NO}_x$  between 20 and 40 km altitude, for various degrees of aerosol loading prior to and following the eruption of Mt. Pinatubo. Profiles of aerosol surface area associated with each MkIV flight originate from Stratospheric Aerosol and Gas Experiment II (SAGE II) analyses of zonal, monthly-mean measurements of extinction [Yue *et al.*, 1994].

## Balloon Measurements

The MkIV Interferometer [Toon, 1991] is the latest solar absorption FTIR spectrometer designed at JPL for the purpose of remotely measuring atmospheric composition. Its high spectral resolution ( $0.01\text{ cm}^{-1}$ ) and broad coverage (650-56X  $\text{cm}^{-1}$ ) allow a large number of gases to be measured simultaneously, including NO,  $\text{NO}_2$ ,  $\text{HNO}_3$ ,  $\text{HNO}_4$ ,  $\text{N}_2\text{O}_5$ ,  $\text{ClNO}_3$ ,  $\text{O}_3$ ,  $\text{N}_2\text{O}$ ,  $\text{N}_2\text{O}_4$ ,  $\text{CH}_4$ ,  $\text{HCl}$ ,  $\text{HOCl}$ , CO, and  $\text{C}_2\text{H}_6$ .

The solar infrared spectra analyzed in this work were acquired during three balloon flights from Fort Sumner, New Mexico ( $34.5^\circ\text{N}, 104.2^\circ\text{W}$ ) on 27 September 1990 and 25 September 1993, and a flight from Daggett, California ( $34.8^\circ\text{N}, 114.8^\circ\text{W}$ ) on 3 April 1993. For the 25 September 1993 flight, volume mixing ratio (vmr) profiles were retrieved from infrared spectra obtained during payload ascent (near nom), as well as sunset and the following sunrise, providing the opportunity to measure the variations of NO and  $\text{NO}_2$  during a daily solar cycle. Only sunset spectra were available for retrieval of vmr profiles for the other flights. An unapodized spectral resolution of  $0.01\text{ cm}^{-1}$  was employed for tangent altitudes above  $\approx 28\text{ km}$ , at which point it was switched to  $0.02\text{ cm}^{-1}$  to allow more rapid sampling, keeping the tangent point separation of successive spectra in the 2 to 3 km range. All flights of the MkIV were accompanied by an *in situ*  $\text{O}_3$  UV photometer. The Submillimeter Limb Sounder (SLS) instrument, which measures  $\text{ClO}$ , OH, and  $\text{HO}_2$  between altitudes of 35 and 50 km by microwave emission spectrometry [Stachnik *et al.*, 1992], flew on the same gondola for the April and September 1993 flights. The Far Infrared Limb Observing Spectrometer (FILOS) instrument, which measures OH between 35 and 45 km by submillimeter spectroscopy [Pickett and Peterson, 1993], accompanied the MkIV 011 the September 1993 flight.

## Data Analysis

The MkIV data analysis consists of two distinct procedures, which are described further in *Sen et al.* [1996]. Briefly, null-linear least squares fitting is first used to calculate the slant column abundance for each target gas in every spectrum. For gases that absorb in more than one spectral interval, a weighted average slant column is calculated. These slant columns, together with the matrix of computed geometrical slant path distances, are then solved to yield concentration profiles. Although the tangent point separation is typically 2 to 3 km at sunset and sunrise, the vmr profiles were retrieved on a 1 km vertical grid. There are two reasons for this choice: (1) to be compatible with the inputs to the spectral calculations and (2) to maintain the high vertical resolution of the limb profiles immediately below the balloon for which tangent point separation is small and of the ascent profile for which the vertical separation between successive spectra was typically only 0.9 km.

The molecular parameters are taken from the ATMOS linelist compilation [*Brown et al.*, 1996], based on HITRAN and updated with new spectroscopic measurements, which incorporate the latest laboratory cross sections for N<sub>2</sub>O<sub>5</sub> [*Cantrell et al.*, 1988], HNO<sub>4</sub> [*May and Friedl*, 1993], and ClNO<sub>3</sub> [*Bell et al.*, 1992]. The estimated uncertainties in the accuracy of the linelist parameters [*Brown et al.*, 1996] used for A<sup>T</sup>O<sub>y</sub> gas retrievals range from 8 to 10% for NO and NO<sub>2</sub>, 15% for ClNO<sub>3</sub>, HNO<sub>3</sub>, N<sub>2</sub>O<sub>5</sub>, and 20% for HNO<sub>4</sub>. The uncertainties for O<sub>3</sub> and N<sub>2</sub>O are  $\approx$ 5%.

The errors of vmr profiles reported in this study represent the  $1\sigma$  measurement precision combined in quadrature with these spectroscopic accuracies. Other systematic error terms such as pointing; and temperature uncertainties are negligible compared with these two: pointing errors have been minimized by fitting temperature insensitive CO<sub>2</sub> lines, and temperature errors minimized by using temperature sensitive CO<sub>2</sub> lines. The measurement precision is calculated during the retrieval process based on considerations such as residuals in spectral fitting. In general, gases with numerous,

strong, well-isolated spectral lines (e.g., O<sub>3</sub>, NO, NO<sub>2</sub>, HNO<sub>3</sub>) yield precisions in their retrieved vmr of typically  $\approx 5\%$  of the peak vmr. Abrams *et al.* [1996] report similar uncertainties in the accuracy of gases measured by ATMOS, obtained also using high-resolution infrared solar occultation spectra.

For NO and NO<sub>2</sub>, whose concentration varies along the line of sight due to the changing solar zenith angle, diurnal correction matrices were calculated by the photochemical model described below for conditions (e.g., temperature, O<sub>3</sub>, appropriate for the occultations [Newchurch *et al.*, 1996]. Figure 1 compares profiles of NO and NO<sub>2</sub> retrieved with (solid line) and without (dashed line) these diurnal corrections. The large fractional validations of NO at sunset result in significant differences between its two profiles, especially below 25 km. However, for NO<sub>2</sub>, whose fractional variation at sunset is smaller, the diurnal correction makes little difference. In fact, less than 10% error is made by ignoring the diurnal variation of NO<sub>2</sub> for altitudes below 25 km. These results are in accordance with previous work on diurnal correction [Boughner, 1980; Roscoe and Pyle, 1987; Russell *et al.*, 1988; Newchurch *et al.*, 1996]. The elements of these correction matrices are simply ratios of calculated concentrations at different solar zenith angles and altitudes. Therefore, the absolute values of model concentrations are not communicated to the retrieval algorithm, and therefore cannot bias the retrieved profiles. From the good agreement achieved between our photochemical model and *in-situ* measurements near the terminator [Salawitch *et al.*, 1994b; Newchurch *et al.*, 1996], we believe that for NO<sub>2</sub>, and for NO above 25 km, the diurnal corrections are not a significant source of uncertainty. The good agreement between diurnally corrected profiles for NO from 18 to 21 km measured by ATMOS and nearly simultaneous *in situ* measurements of NO suggests the diurnal correction procedure yields accurate retrievals at altitudes above 18 km [Newchurch *et al.*, 1996].

## Photochemical Model

The photochemical model has been used previously in many stratospheric studies [e.g., *McElroy et al., 1992*]. Reaction rates and absorption cross sections are adopted from the JPL 94-26 compendium [*DeMore et al., 1994*]. The abundance of radical (i.e., NO, NO<sub>2</sub>, OH, HO<sub>2</sub>, ClO, BrO) and reservoir (i.e., HNO<sub>3</sub>, HCl, N<sub>2</sub>O<sub>5</sub>, ClNO<sub>3</sub>) gases has been calculated allowing for diurnal variation and assuming a balance between production and loss rates of each species integrated over a 24 hour period, for the latitude and temperature of the observations. Concentrations of precursors (i.e., O<sub>3</sub>, H<sub>2</sub>O, CH<sub>4</sub>, CO, C<sub>2</sub>H<sub>6</sub>), the total abundance of NO<sub>y</sub>, and Cl<sub>y</sub> ( $\approx$  HCl + ClO + HOCl + ClNO<sub>3</sub>) are constrained to match observations of MkIV and SLS, which measured ClO from the same gondola. The temperature profile was obtained from the MkIV analysis of temperature sensitive CO<sub>2</sub> absorptions, and for September 1993 equaled 216, 222, and 230 K at 22, 26, and 32 km, respectively. The input O<sub>3</sub> profile is based on observations by MkIV, S1,S, and an *in situ* UV photometer (Figure 2) and is discussed in detail by *Osterman et al. [1997]*.

All heterogeneous reactions on sulfate aerosols believed to affect partitioning of stratospheric NO<sub>y</sub> and Cl<sub>y</sub> at mid-latitudes were included in the model. Heterogeneous hydrolysis of N<sub>2</sub>O<sub>5</sub> was assumed to occur with a reaction probability of 0.1 [*DeMore et al., 1994*]; the formulation of *Hanson et al. [1996]* was used for the heterogeneous rate of BrNO<sub>3</sub> + H<sub>2</sub>O; and the formulations of *Ravishankara and Hanson [1996]* were used for the remaining sulfate heterogeneous reactions (HCl + ClNO<sub>3</sub>, HOCl + HCl, and ClNO<sub>3</sub> + H<sub>2</sub>O). Kinetic parameters for HOBr -t HCl heterogeneous reaction are from *Hanson and Ravishankara [1995]*. Profiles of aerosol surface area originate from zonal, monthly-mean observations of SAGE II [*Yue et al., 1994*].

## Results and Discussion

Accurate measurements of ozone are a prerequisite for quantifying our understanding of nitrogen oxides. Not only does  $O_3$  directly affect the  $NO/NO_2$  and  $NO_2/HNO_3$  ratios, but it also influences many other radicals (e.g.,  $C1O$ ,  $OII$ ) that interact with  $NO_x$  and  $NO_y$ . Figure 2 shows a comparison of the sunset profile of ozone measured by MkIV on 25 September 1993, and ascent and descent profiles observed by the *in situ* UV sensor on board the same gondola. The two *in situ* measurements of  $O_3$ , obtained  $\approx 20$  hours apart and separated by 200 km, agree to better than 5%. This indicates relatively quiescent conditions in the stratosphere during the time of observation, typical for 35°N during fall. The excellent agreement between the *in situ* and remote observations of  $O_3$ , better than 6% for all altitudes above 20 km, provides confidence the  $O_3$  profile is not a major source of uncertainty in the model calculations of the apportionment of nitrogen oxides into member species. Since all the gases measured by MkIV are analyzed with the same spectral fitting and retrieval algorithms, the good agreement for  $O_3$  and also for  $N_2$  lends confidence that the other gases, for which no direct validation is possible, are also retrieved accurately. The excellent agreement between ATMOS (using a measurement and data analysis technique similar to MkIV) and *in situ* measurements of  $N_2O$ ,  $CH_4$ ,  $H_2O$ ,  $NO_y$ ,  $O_3$ , CFC11, CFC12,  $CCl_4$ , and  $SF_6$  further demonstrate the accuracy achievable by the solar occultation technique [Chang *et al.*, 1996a,b].

### $NO_y$ Partitioning and Budget

Observed and theoretical vmr profiles of  $NO_y$  species at sunset are illustrated in Figure 3. Profiles for  $N_2O_5$  at sunrise are also shown. Calculated profiles of  $NO_y$  species not observed by MkIV ( $NO_3$ ,  $BrNO_3$ , and  $HNO_2$ ) make only small contributions to the total budget, and are therefore not shown. Overall, the agreement between observed and calculated profiles for all  $NO_y$  species is good. The only significant systematic disagreement is for  $NO_2$  below 28 km, where measured values exceed calculated values

by up to 30%. For most of this altitude range, there is good agreement (better than 10%) between observed and calculated vmrs of NO and HNO<sub>3</sub>. Consequently, the observed ratios NO<sub>2</sub>/NO and NO<sub>2</sub>/HNO<sub>3</sub> exceed theoretical estimates below 28 km. The apparent disagreement between observed and modeled NO at 20 km could result from an imperfect diurnal correction, which is not included in our estimate of the error bars and could be very large at this altitude.

The comparisons shown in Figure 3 demonstrate good understanding of most reactive and photolytic processes that regulate the abundance of nitrogen oxides, particularly for altitudes above 28 km. The observed buildup of N<sub>2</sub>O<sub>5</sub> during the night as well as its value at the evening terminator are simulated accurately, suggesting the coupling between NO<sub>x</sub> and HNO<sub>3</sub> is being treated in a realistic manner by the model. The range of altitudes for which NO, NO<sub>2</sub>, and HNO<sub>3</sub> are calculated to be the dominant species of the NO<sub>y</sub> family agrees with observations, as does the concentration of each gas for these altitudes. This suggests the height dependence of the concentration of atomic oxygen and the photolysis rate of NO<sub>2</sub> are represented accurately by the model above 28 km, and the production and loss processes for HNO<sub>3</sub> are represented accurately at lower altitudes. The proper treatment of HO<sub>x</sub> above 28 km is supported by the agreement between observe.cl and theoretical profiles of NO<sub>2</sub> and HNO<sub>4</sub> (produced by the reaction of NO<sub>2</sub> with HO<sub>2</sub>), as well as comparisons with vmrs of OH and HO<sub>2</sub> observed by different instruments from the same gondola [Pickett and Peterson, 1996; Osterman et al., 1997].

Two simulations of ClNO<sub>3</sub> are illustrated in Figure 3. The nominal case (solid line) assumes a 7% yield of HCl from ClO + OH and the Michelsen *et al.* [1994] formulation for the quantum yield of O(<sup>1</sup>D) from O<sub>3</sub> photolysis, while the other (dashed line) assumes a 0% HCl yield and the DeMore *et al.* [1994] formulation of O(<sup>1</sup>D) quantum yield. Only the nominal case is shown for simulations of other species, since calculated profiles are insensitive to the choice of these two kinetic parameters. The vmr profile

of  $\text{ClNO}_3$  observed by MkIV generally lies between the two theoretical calculations. A 7% yield of HCl was reported to be consistent with: (1) ATMOS observations of HCl and  $\text{ClNO}_3$  [Michelsen *et al.*, 1996], (2) FIRS-2 measurements of HCl and HOCl obtained during 26 September 1989 [Chance *et al.*, 1996], and (3) SLS measurements of ClO during the September 1993 balloon flight [Osterman *et al.*, 1997]. While the MkIV measurements are not inconsistent with a 7% yield of HCl, they suggest a smaller yield for reasons not fully understood [Jaeglé, 1995].

The photochemical model simulation shown in Figure 3 have been constrained to match the total amount of  $\text{NO}_y$  measured by MkIV at each altitude, as discussed above in the model description section. MkIV also obtains simultaneous measurements of the concentration profile of  $\text{N}_2\text{O}$ , the source of  $\text{NO}_y$ . Figure 4 illustrates the relation between  $\text{NO}_y$  and  $\text{N}_2\text{O}$  observed by MkIV, as well as the relation measured by *in situ* instruments aboard the ER-2 aircraft at northern mid-latitudes during February and November, 1994. The *in situ* determination of  $\text{NO}_y$  is ascribed a  $1\sigma$  total uncertainty of better than 10% [Fahey *et al.*, 1989], while the *in situ* measurement of  $\text{N}_2\text{O}$  has an estimated  $1\sigma$  total uncertainty of 3% [Locowenstein *et al.*, 1989]. Theoretically,  $\text{NO}_y$  and  $\text{N}_2\text{O}$  are expected to exhibit a compact, near linear relation in the lower stratosphere since the rate for redistribution by transport is short compared to photochemical production and loss of each quantity [Plumb and Ko, 1992]. The two measurements of  $\text{NO}_y$  versus  $\text{N}_2\text{O}$  agree to within the uncertainty of the observations: each is consistent with a slope of  $-0.07$  for  $160 < \text{N}_2\text{O} < 310$  ppbv, similar to two dimensional model simulations [Keim *et al.*, 1997]. These comparisons corroborate the accuracy of the MkIV retrievals of the major  $\text{NO}_y$  species (e.g.,  $\text{HNO}_3$ ,  $\text{NO}_2$ , and NO) for the altitudes at which they are dominant. Furthermore, the MkIV relation also illustrates the decrease of  $\text{NO}_y$  with decreasing  $\text{N}_2\text{O}$  at altitudes above 33 km, due to the rapid (with respect to transport) loss of  $\text{NO}_y$  by the reaction of  $\text{N} + \text{NO}$ .

## NO<sub>x</sub> Chemistry

The reactions [*Crutzen, 1970; Johnston, 1971*]



constitute the primary chemical loss process for stratospheric ozone between altitudes of approximately 24 to 36 km [e.g., *Jucks et al., 1996; Osterman et al., 1997*]. Understanding the processes that regulate NO, NO<sub>2</sub>, and NO<sub>x</sub> is central to understanding the chemistry of stratospheric O<sub>3</sub>. Loss of NO occurs primarily by reaction (1), with a small contribution from



Removal of NO<sub>2</sub> occurs mainly by

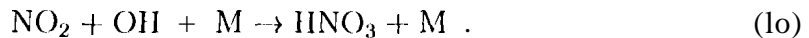
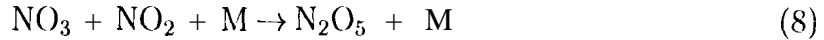
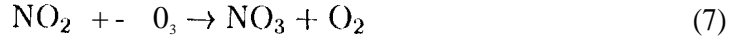


which is much faster than loss by reaction (2) for altitudes below 35 km. Since production and loss of NO and NO<sub>2</sub> occur rapidly, the ratio of the concentration of these species is expected to be described by the instantaneous value of

$$\frac{\text{NO}}{\text{NO}_2} = \frac{J_{\text{NO}_2}}{(k_1 \cdot [\text{OS}] + k_4 \cdot [\text{m}])} \quad (6)$$

where J<sub>NO<sub>2</sub></sub> is the photolysis rate of NO<sub>2</sub>, and k<sub>1</sub> and k<sub>4</sub> are rate constants for the respective reactions.

Changes in  $\text{NO}_x$  occur much more slowly than the time for equilibration of  $\text{NO}$  and  $\text{NO}_2$ . Removal of  $\text{NO}_x$  occurs mainly by production of  $\text{N}_2\text{O}_5$  and  $\text{HNO}_3$ :



Resupply of  $\text{NO}_x$  occurs by photolysis of  $\text{N}_2\text{O}_5$  and  $\text{HNO}_3$ , and by reaction of  $\text{HNO}_3$  with  $\text{OH}$ . Between altitudes of 26 and 40 km, changes in the concentrations of  $\text{NO}_x$  and  $\text{N}_2\text{O}_5$  are expected to exhibit a 2:1 stoichiometry, because  $\text{N}_2\text{O}_5$  is the dominant nighttime reservoir of  $\text{NO}_x$ . At lower altitudes, the stoichiometry is expected to exceed 2:1 because, even though reaction (9) is the dominant process by which  $\text{NO}_x$  is converted to  $\text{HNO}_3$  [e.g., *McElroy et al.*, 1992; *Faherty et al.*, 1993], a fraction of  $\text{NO}_x$  is converted to  $\text{HNO}_3$  by reaction (10).

MkIV observations of  $\text{NO}_x$  and  $\text{N}_2\text{O}_5$  test our understanding of the diurnal variation of reactive nitrogen. Measured concentrations of  $\text{NO}_x$  and  $\text{N}_2\text{O}_5$  at sunrise and sunset for three altitudes are shown in Figure 5. Also shown are midday measurements of  $\text{NO}_x$ , obtained during balloon ascent and retrieved using the same procedures as the sunset and sunrise profiles, taking into account the fundamental difference in observation geometry. The midday profile of  $\text{N}_2\text{O}_5$  could not be retrieved since the airmass was too small to provide sufficient absorption in ascent spectra.

Theoretical curves for the diurnal variation of  $\text{NO}_x$  and  $\text{N}_2\text{O}_5$  are shown also in Figure 5. The solid curves are results of independent simulations constrained by

measured concentrations of precursors at sunset, (red line) and sunrise (blue line), assuming a cloud-free atmosphere with an albedo of 0.24. The shaded region indicates the sensitivity of model results to variations in albedo: highest values of  $\text{NO}_x$  are calculated assuming high altitude, highly absorbing clouds (albedo=0.2), while lowest values are found assuming highly reflecting clouds (albedo=0.8). Changes in albedo were allowed to impact all photolytic processes (e.g.,  $J_{\text{NO}_2}$ , which affects the  $\text{NO}/\text{NO}_2$  ratio on rapid time scales, as well as  $J_{\text{HNO}_3}$ , which affects  $\text{NO}_x/\text{HNO}_3$  on longer time scales) and is meant to quantify, in a simple manner, the uncertainty of model results associated with the photolytic environment experienced by air parcels during the observation and days immediately prior to it. The atmosphere was cloud free in the MkIV field of view when the sunset spectra were obtained (spectra were recorded for tangent heights as low as 6 km), but contained high-altitude thunderstorm clouds during sunrise.

The results shown in Figure 5 demonstrate a fundamentally good understanding of the coupling between stratospheric  $\text{NO}_x$  and  $\text{N}_2\text{O}_5$ . Observed values of  $\text{NO}_x$  and  $\text{N}_2\text{O}_5$  agree with theory at 32 km, to within the measurement and model uncertainties. Similarly, observed values of  $\text{NO}_x$  at sunrise and  $\text{N}_2\text{O}_5$  at sunset for 26 km agree with model values. However, at this altitude observations of both  $\text{NO}_x$  at midday and sunset as well as  $\text{N}_2\text{O}_5$  at sunrise exceed model values, although theory and observation slightly overlap given the respective uncertainties. MkIV observations of variations in concentrations of  $\text{NO}_x$  and  $\text{N}_2\text{O}_5$  at both 26 and 32 km exhibit the expected 2:1 stoichiometry. During sunset at 22 km, observation of  $\text{NO}_x$  exceed theory, and  $\text{N}_2\text{O}_5$  is less than theory, by amounts roughly consistent with the expected stoichiometry.

As discussed previously the only significant discrepancy in this study is the tendency of observed  $\text{NO}_2$  to exceed model values below 28 km (e. g., Figure 3). The strong and well defined infrared absorptions of  $\text{NO}_2$  make it one of the more easily measured gases in the MkIV spectra. Two separate bands at 1600 and  $2900 \text{ cm}^{-1}$  are used to retrieve  $\text{NO}_2$  and the resulting profiles are consistent to better than 10% for all altitudes, and

better than 5% below 27 km. The profile of NO<sub>2</sub> shown in Figure 3 is a weighted average of retrievals from both bands. The good agreement between measured and calculated NO<sub>2</sub> above 30 km, where pressure broadening of the NO<sub>2</sub> absorption features is negligible, indicates that errors in the NO<sub>2</sub> line strengths are unlikely to be the cause of the discrepancy at lower altitudes. A 40% increase in the pressure-broadened half-widths (PBHW) of the NO<sub>2</sub> lines would greatly improve the agreement between calculated and measured NO<sub>2</sub>, since its effect on retrieved vmr would increase with pressure. However, this increase exceeds the 15% uncertainty of the PBHW estimated from laboratory measurements [Brown *et al.*, 1996]. Recent laboratory measurements of the PBHW of NO<sub>2</sub> (D. Newnham, RAL, personal communication, 1997) indicate that the actual values may be 10 to 15% larger than those used in this analysis. Although this would decrease the retrieved MkIV NO<sub>2</sub> concentrations in the lower stratosphere by  $\approx$ 10%, a significant disagreement would still remain.

Our estimate of the total uncertainty of the MkIV measurement of NO<sub>2</sub> varies from 19% at 20 km to 11 % at 30km. Therefore, the discrepancy between observations and theory is significant below 28 km. Additionally, NO and HNO<sub>3</sub> are measured with sufficient accuracy and precision in the lower stratosphere that the discrepancy between theory and observation of NO/NO<sub>2</sub> and NO<sub>2</sub>/HNO<sub>3</sub> is also larger than the measurement uncertainty below 28 km.

Figure 6 illustrates co-located measurements of NO, NO<sub>2</sub> and their ratio by HALOE (Version 18, 33.6°N, 11 0°W) 24 hours earlier and 100 km distant from the MkIV observations on 25 September 1993. The HALOE measurements of NO are based on absorption in the 1900 cm<sup>-1</sup> band, the same as used by the MkIV. The HALOE measurements of N O<sub>2</sub> are based on absorption in the 1600 cm<sup>-1</sup> band, one of the two bands used in the MkIV analysis. The estimated total uncertainties of individual retrievals of NO and NO<sub>2</sub> by HALOE are 40% and 26%, respectively, at 22 km [Gordley *et al.*, 1996, Figures 7 and 8]. The measurements of NO, NO<sub>2</sub> and their ratio by the

two remote sensing instruments agree to within 10% above 27 and 25 km, respectively. Theoretical profiles are also shown in Figure 6. Between 23 and 34 km, the MkIV and HALOE measurements of NO<sub>2</sub> are both larger than the model values. Below 23 km, the larger uncertainties associated with the measurements make it difficult to draw any definitive conclusions.

The disagreement between NO<sub>2</sub> measured by MkIV and the calculated values exhibits a similar pattern with respect to altitude for all balloon flights analyzed to date, as shown in Figure 7. These flights sampled air with substantially different levels of aerosol loading, reflecting the relatively clean period prior to the eruption of Mt. Pinatubo, and the subsequent build-up and decline of volcanic aerosol. This suggests the NO<sub>2</sub> discrepancy is not related to transient phenomena such as the possible effect of Mt. Pinatubo aerosol on the photolysis rate of NO<sub>2</sub>. Recent ATMOS measurements obtained in November 1994 at high southern latitudes with relatively low aerosol loading reveal a similar pattern of excess NO<sub>2</sub> with respect to model profiles [Rinsland *et al.*, 1996, Figure 3]. Similarly, nighttime measurements of NO<sub>2</sub> obtained by UV-Vis spectroscopy in March 1994 at 44° N latitude also exhibit an excess over calculated values in the 22 to 28 km altitude range [Renard *et al.*, 1997]. However, an analysis of earlier ATMOS observations obtained at mid-latitudes during April/May 1985 does not reveal a similar discrepancy for NO<sub>2</sub> [e.g., McElroy *et al.*, 1992, Figures 10 and 12].

Figure 8 illustrates the variation with respect to solar zenith angle of MkIV observations of NO, NO<sub>2</sub>, and the NO/NO<sub>2</sub> ratio at altitudes of 32, 26, and 22 km. The model simulations are similar to those shown in Figure 5, for sunset (red line) and sunrise (blue line) constraints and a cloud-free albedo of 0.24. The shaded regions represent the sensitivity of calculated values to variations in albedo as discussed previously. The observed concentrations of NO agree with theory, to within the measurement and model uncertainty, at all altitudes and times except for 26 km at sunrise. However, the precision of the midday observations of NO is poor below 26 km owing to the low air

mass factor of the ascent spectra. Similarly, the noontime measurements of NO<sub>2</sub> below 27 km are not sufficiently accurate or consistent to ascertain whether they agree better with the model, or with the 20-30% excess over the model values at sunrise and sunset.

The observed NO/NO<sub>2</sub> ratio is lower than model values at sunrise and sunset for altitudes below 26 km (Figure 8). The calculated photolysis rate of NO<sub>2</sub> agrees well with photolysis rates inferred from observations of the direct and diffuse flux of radiation between 300 to 775 nm from the ER-2 aircraft [McElroy *et al.*, 1995] for solar zenith angles as high as 80° at 20 km [Gao *et al.*, 1997, Figure 4]. Therefore the photolysis rate of NO<sub>2</sub> is unlikely to cause the discrepancy in NO/NO<sub>2</sub> ratio illustrated in Figure 8. Since loss of NO at 22 km by reaction with O<sub>3</sub> proceeds at a rate about four times faster than loss by reaction with ClO, and theory and observation of ClO are in reasonable agreement [Avallone *et al.*, 1993; Salawitch *et al.*, 1994a; Chang *et al.*, 1996a], it is unlikely that uncertainties in the kinetics of reaction (4) or in the abundance of ClO will resolve the dilemma posed by the observations of NO/NO<sub>2</sub>.

Figure 9 illustrates the recommended value for the rate constant of the reaction NO + O<sub>3</sub> from the JPI compendium, as well as its nominal 1 $\sigma$  uncertainty [DeMore *et al.*, 1994] as a function of inverse temperature. Also shown are individual laboratory measurements used in the determination of the recommended rate. The recommended uncertainty of the rate is  $\approx$ 50% for a temperature of 220 K [DeMore *et al.*, 1994], considerably larger than the standard deviation about the mean of the individual measurements at this temperature. Also shown is the reaction rate required to balance, in the absence of any other kinetic changes, the NO/NO<sub>2</sub> ratio observed by MkIV at sunset. We do not intend to imply by this figure that rate constants can be determined from atmospheric measurements. It is merely a way of illustrating the uncertainty in the model calculation, and its relationship to laboratory and atmospheric observations. The rate required to balance the observed NO/NO<sub>2</sub> ratio below 23 km is larger than allowed by the laboratory observations, and consequently uncertainties in this rate are an

unlikely explanation for the observed ratio at the lowest altitudes. However, it is difficult to rule out, the possibility, based on the individual laboratory measurements, that the true rate of reaction (1) is 20% faster than the recommended value for temperatures near 216 K, which would explain the measured NO/NO<sub>2</sub> ratios at sunrise and sunset between altitudes of 24 to 32 km.

*In situ* observation from the ER-2 aircraft of NO (by chemiluminescence) and NO<sub>2</sub> (by chemiluminescence and by a '1'111,S) at mid-latitudes obtained during SPADE (May 1993) indicated a discrepancy between theory and observation of the NO/NO<sub>2</sub> ratio near 20 km during midday of  $\approx 35\%$  [Jacqué *et al.*, 1994], *but in the opposite sense* of the discrepancy noted for the MkIV occultations. However, more recent measurements of NO and N(3<sub>z</sub>), obtained at mid-latitudes near 20 km during ASHOE/MAESA (February to November, 1994) using the *in situ* chemiluminescence detector, agree with the theoretical ratio to better than 8% [Gao *et al.*, 1997].

The MkIV observations suggest a discrepancy in our understanding of the NO/NO<sub>2</sub> ratio. For illustrative purposes only, we have calculated the abundance of NO<sub>y</sub> gases at 22 km allowing for a 40% reduction in J<sub>NO<sub>2</sub></sub> at all solar zenith angles, which forces agreement with the measured NO/NO<sub>2</sub> ratio. Results shown in Figure 8 indicate that, even though the NO/NO<sub>2</sub> ratio is simulated correctly, the model values of both NO and NO<sub>2</sub> remain significantly lower than observation. To simultaneously match constraints posed by MkIV observations of NO/NO<sub>y</sub>, NO<sub>2</sub>/NO<sub>y</sub>, and NO/NO<sub>2</sub> at 22 km requires not only a reduction in J<sub>NO<sub>2</sub></sub> (or, equivalently, an increase in k<sub>1</sub>), but also either a reduction in the rate of the heterogeneous hydrolysis of N<sub>2</sub>O<sub>5</sub> [reaction (1 O)] from the recommended reaction probability of 0.1 [DeMore *et al.*, 1994] to a value as low as 0.02, or else accelerated removal of HNO<sub>3</sub>.

Lary *et al.* [1997] have postulated that heterogeneous processes occurring on the surface of carbonaceous soot particles may convert HNO<sub>3</sub> to NO<sub>2</sub>. If this process could act rapidly enough to compete with the loss of NO<sub>x</sub> by reaction (1 O), it would offer an

explanation for the tendency of the MkIV observations of  $\text{NO}_2$  to exceed model values. However, this reaction would cause serious difficulties in accounting for a wealth of observations of the  $\text{NO}/\text{NO}_y$  ratio obtained from the ER-2 [Salawitch *et al.*, 1994a,b; Gao *et al.*, 1997] as well as our observation of the  $\text{NO}/\text{HNO}_3$  ratio above 22 km. Simultaneous measurements of NO and  $\text{NO}_2$  by instruments on the ER-2 and MkIV for the same air masses during the upcoming POLARIS campaign will hopefully shed additional light on our understanding of the processes that regulate  $\text{NO}_x$ .

### The effect of Mt. Pinatubo aerosols on $\text{NO}_x$

Increases by factors of 20 to 30 in the surface area of sulfate aerosol following the June 1991 eruption of Mt. Pinatubo [e.g., McCormick *et al.*, 1995] reduced levels of  $\text{NO}_x$  throughout the stratosphere due to reaction (10), the heterogeneous hydrolysis of  $\text{N}_2\text{O}_5$  [e.g., Fahey *et al.*, 1993; Webster *et al.*, 1994]. The reduction in  $\text{A}^{\text{T}}\text{OX}$  led to increases in concentrations of  $\text{ClO}$  and  $\text{HO}_x$ , increasing the overall efficiency of catalytic removal of  $\text{O}_3$  by reactive nitrogen, chlorine, and hydrogen species in the lower stratosphere [e.g., Kinnison *et al.*, 1994; Rodriguez *et al.*, 1994]. Previous analyses of observations of NO and  $\text{NO}_y$  from the ER-2 [Fahey *et al.*, 1993; Kawa *et al.*, 1993; Salawitch *et al.*, 1994a,b; Gao *et al.*, 1997] suggested that reaction (10) is the dominant sink for  $\text{NO}_x$  throughout much of the lower stratosphere following the eruption of Mt. Pinatubo. Similar conclusions were reached based on analysis of balloon-borne observations of  $\text{NO}_2$  and  $\text{HNO}_3$  [Webster *et al.*, 1994] as well as NO and  $\text{NO}_y$  [Kondo *et al.*, 1997]. However, Koike *et al.* [1994] observed larger increases in the column abundance of  $\text{HNO}_3$ , and decreases in column  $\text{NO}_2$ , than could be accounted for by reaction (10) alone. The variation of *in situ* observations of HCl with aerosol surface area has been interpreted as evidence for a dominant influence by heterogeneous reactions involving HCl and  $\text{ClNO}_3$  [Webster *et al.*, 1997]. Furthermore, Solomon *et al.* [1996] showed that the observed decline in  $\text{O}_3$  during the past several decades, due to both the build up of chlorine! from

industrial CFCs and changes in sulfate aerosol loading, was about 50% larger than calculated by their two-dimensional model. Similarly, *Kinnison et al.*[1994] are unable to account for the magnitude of the observed reduction of O<sub>3</sub> following the eruption of Mt. Pinatubo when both the radiative and chemical affects of volcanic aerosol are considered.

We present observations of NO, NO<sub>2</sub>, and NO<sub>y</sub> by MkIV for three balloon flights encountering vastly different levels of sulfate aerosol loading. These observations provide a test of our understanding of the heterogeneous chemistry associated with Mt. Pinatubo aerosols on the NO<sub>x</sub>/NO<sub>y</sub>ratio. We seek to establish whether the observations provide evidence that other heterogeneous sinks of NO<sub>x</sub> besides reaction (10) exert a substantial influence on the chemistry of the mid-latitude stratosphere. If so, loss of O<sub>3</sub> due to Mt. Pinatubo aerosols would likely exceed model predictions [e.g., *Prather*, 1992].

Figure 10 compares the measured profiles of NO<sub>x</sub>/NO<sub>y</sub> at sunset to theoretical profiles for flights of MkIV during September 1990, April 1993, and September 1993. Also shown are the profiles of sulfate aerosol surface area associated with each MkIV flight, derived from SAGE II zonal, monthly-mean measurements of extinction in the visible and near ultraviolet [*Yue et al.*, 1994]. The theoretical curves are constrained by profiles of O<sub>3</sub>, H<sub>2</sub>O, CH<sub>4</sub>, NO<sub>y</sub>, HCl + ClNO<sub>3</sub> → HOCl, temperature, etc. measured by MkIV for each flight and the SAGE II surface area profile shown in Figure 10. Three model curves for NO<sub>x</sub>/NO<sub>y</sub> are shown for each flight: results of (1) a purely gas phase calculation (solid line), (2) gas phase + N<sub>2</sub>O<sub>5</sub> hydrolysis (reaction 10) only (dotted line), and (3) gas phase -t- all heterogeneous reactions (dashed line). Calculated values of the NO<sub>x</sub>/NO<sub>y</sub> ratio are nearly identical for the two heterogeneous simulations because temperatures encountered during the three flights were too warm (209.1, 211.0, and 209.1 K at 20 km for September 1990, April 1993, and September 1993) and aerosol surface areas too low for loss of NO<sub>x</sub> by the two heterogeneous reactions involving

$\text{ClNO}_3$  [e.g., *Ravishankara and Hanson, 1996*]. The small difference between the two heterogeneous simulations is predominantly due to the reaction of  $\text{BrNO}_3 + \text{H}_2\text{O}$ . This reaction does not become an efficient sink of  $\text{A}^{\text{T}}\text{OX}$  for levels of aerosol loading encountered during April 1993 and contemporary levels of  $\text{Br}_y$  [e.g., 17.9 pptv at 22 km for April 1993] until air parcels reach latitudes poleward of  $50^\circ$ , where the less intense photolytic environment results in slower rates for competing processes [*Tie and Brasseur, 1996*].

The height dependence of the observed  $\text{NO}_x/\text{NO}_y$  ratio agrees fairly well with profiles calculated using the heterogeneous models, although the observed ratio exceeds theory between altitudes of 23 and 30 km. For this range of altitudes, the observations agree more closely, in general, with the ‘gas phase only’ calculations. For altitudes below 23 km, measured values of this ratio agree well with the ‘heterogeneous’ simulations and are appreciably smaller than the ‘gas phase only’ calculations, consistent with conclusions of numerous previous studies [e. g., *McElroy et al., 1992; Dessler et al., 1993; Fahey et al., 1993; Webster et al., 1994; Hoymo et al., 1997*].

It is tempting to contemplate the existence of a neglected process that converts  $\text{HN}_3$  to  $\text{NO}_x$ , such as heterogeneous reactions on soot as suggested by Lary et al. [1997], based on the comparisons shown in Figure 10. Likewise, a large reduction in the rate of reaction (10) would also yield better agreement between theory and observation of  $\text{NO}_x/\text{NO}_y$  between 23 and 30 km. However, the observation of excess  $\text{NO}_x$  relative to the ‘heterogeneous’ model profiles is caused primarily by the discrepancy in  $\text{NO}_2$ , as discussed previously. The observed  $\text{NO}/\text{HNO}_3$  ratio in this altitude range agrees well with profiles calculated using published rates for the heterogeneous reactions listed above [e.g., Figure 3]. Furthermore, the ‘heterogeneous’ model profiles of  $\text{NO}_x/\text{NO}_y$  agree with observed values below 23 km, even though the observed  $\text{NO}/\text{NO}_2$  ratio is simulated poorly [e. g., Figure 8]. Understanding the cause of the discrepancy between theory and observation of the  $\text{NO}/\text{NO}_2$  ratio, which should be in near instantaneous

equilibrium with the value of expression (5), is a prerequisite for gaining further insight into the apparent disagreement for  $\text{NO}_x/\text{NO}_y$  between 23 and 30 km.

Figure 11 quantifies the dependence of the  $\text{NO}_x/\text{NO}_y$  ratio on aerosol surface area for each flight,. The model curves are identical to those shown in Figure 10. Aerosol surface area is used as the abscissa for all model results, even though it has little bearing on the gas phase simulation. The gas phase calculation captures the non-linear dependence of the observed  $\text{NO}_x/\text{NO}_y$  ratio for surface area less than  $\approx 0.6 \mu\text{m}^2\text{cm}^{-3}$ , primarily due to the influence of  $\text{O}_3$ , and consistently overpredicts the magnitude of the ratio at larger values of surface area. The abundance of  $\text{O}_3$  controls both the apportionment of  $\text{NO}_x$  between  $\text{NO}$  and  $\text{NO}_2$  and the nighttime formation of  $\text{N}_2\text{O}_5$ . Since the nighttime formation of  $\text{N}_2\text{O}_5$  occurs by the reaction of  $\text{NO}_2$  and  $\text{NO}_3$  (i.e., quadratically dependent on  $\text{NO}_x$ ), the  $\text{NO}_x/\text{NO}_y$  ratio is expected to eventually become insensitive to increases in surface area beyond a critical value, provided  $\text{N}_2\text{O}_5 + \text{H}_2\text{O}$  is the dominant sink for  $\text{NO}_x$ . The calculations in Figure 11 suggest this critical value is  $\approx 4 \mu\text{m}^2\text{cm}^{-3}$  for the conditions encountered during the balloon flights. This critical value together with the  $\text{NO}_x/\text{NO}_y$  ratio at saturation are consistent with previous balloon and airborne chemiluminescence observations of  $\text{NO}$  and  $\text{NO}_y$  [Dessler *et al.*, 1993; Fahey *et al.*, 1993; Kondo *et al.*, 1997] and suggest  $\text{N}_2\text{O}_5 + \text{H}_2\text{O}$  is the dominant sink of  $\text{NO}_x$  for the sampled air masses.

## Conclusions

Observations obtained at mid-latitude ( $35^\circ\text{N}$ ) during the September 1993 balloon flight of the JPL MkIV interferometer, and aerosol surface area basin] on SAGE II extinction measurements, have been examined to assess our understanding of the  $\text{NO}_y$  budget and partitioning of  $\text{NO}_y$  species. The variation of the total nitrogen content for the individual  $\text{NO}_y$  species relative to  $\text{N}_2\text{O}$  agrees well with *in situ* observations and previously published relations found using two dimensional models. The MkIV

observations provide an important test for models since they extend to considerably higher altitudes than the *in situ* observations.

MkIV observations of NO, NO<sub>2</sub>, and HNO<sub>3</sub> agree well with theoretical profiles for the range of altitudes that each gas is the dominant NO<sub>y</sub> species. Our observations of the diurnal variation of NO<sub>x</sub> and N<sub>2</sub>O<sub>5</sub> exhibit close agreement with the theoretical stoichiometry between 20 and 40 km, suggesting the coupling between NO<sub>x</sub> and its dominant, nighttime reservoirs is well understood. Measured vmr profiles of all NO<sub>y</sub> species agree well with model profiles, except that, the observed abundance of NO<sub>2</sub> in the lower stratosphere exceeds calculated values by 20 to 30%. The resulting discrepancies between theory and observation of the NO/NO<sub>2</sub> and NO<sub>2</sub>/HNO<sub>3</sub> ratios for altitudes between 20 and 28 km are larger than the estimated total uncertainty (accuracy and precision) of the measurements. Published uncertainties in laboratory measurements of the absorption cross section of NO<sub>2</sub> [DeMore *et al.*, 1994] and the rate of NO + O<sub>3</sub> are individually smaller than the discrepancy for the NO/NO<sub>2</sub> ratio below 23 km. However, a 10% increase in the rate of NO + O<sub>3</sub> at cold temperatures, together with a 10% increase in the pressure-broadened half-widths of the NO<sub>2</sub> lines, both of which appear plausible, would lead to substantial improvement in agreement between observed and calculated NO<sub>2</sub> in the lower stratosphere, but still leave a difference of  $\approx$ 10%.

The comparison between observation and theory for three MkIV balloon flights before (September 1990) and after (April and September 1993) the eruption of Mt. Pinatubo suggests that N<sub>2</sub>O<sub>5</sub> hydrolysis alone can describe the observed NO<sub>x</sub>/NO<sub>y</sub> ratio. Additional heterogeneous reactions do not perturb this ratio appreciably for surface area below  $14 \text{ cm}^{-2}$  for the temperatures (209 to 219 K) of our mid-latitude observations. Our analysis of these observations suggests heterogeneous reactions involving ClNO<sub>3</sub> and HCl are not a significant sink for mid-latitude NO<sub>x</sub>, which had been a possible explanation for the quantitative anomalies of column NO<sub>2</sub> and HNO<sub>3</sub> presented by Koike *et al.* [1994]. The observed saturation of NO<sub>x</sub>/NO<sub>y</sub> ratio limits

the increase of ClO within the Cl<sub>y</sub> reservoir. *Osterman et al.* [in preparation] show that MkIV observations of HCl and ClNO<sub>3</sub> at 20 km obtained during the same flights are relatively insensitive to surface area, providing further evidence that heterogeneous reactions involving ClNO<sub>3</sub> and HCl do not proceed rapidly enough to significantly alter NO<sub>x</sub> or ClO for the sampled air masses. Our observations suggest the decline in reactive nitrogen by volcanic aerosol is well understood and that catastrophic loss of O<sub>3</sub> due to massive enhancements in ClO [e.g., *Prather*, 1992] and large reductions in HCl [*Webster et al.*, 1997] is unlikely for the environmental conditions encountered by these balloon flights.

**Acknowledgments.** The authors wish to thank D.C. Petterson, J.H. Riccio, R.D. Howe, and W. Il. Wilson of JPL for their considerable field support during the balloon campaign. We wish to thank the NSBF which conducted the balloon launches, flight operations and recovery of the payload. We also wish to thank D. W. Fahey (NOAA) for the use of the ER-2 NO<sub>y</sub> data, M. Loewenstein (NASA/AMES) for the use of the ER-2 N<sub>2</sub>O data, and J.M. Russell, 111 (Hampton University) for the use of the HALOE NO and NO<sub>2</sub> measurements. This research was performed at Jet Propulsion laboratory, California Institute of Technology, under contract with the National Aeronautics and Space Administration.

## References

- Abrams, M.C. *et al.*, on the assessment and uncertainty of atmospheric trace gas measurements with high resolution infrared solar occultation spectra from space by the ATMOS experiment, *Geophys. Res. Lett.*, 23, 2337-2340, 1996.
- Avallone, L. M., D.W. Toohey, W.H. Brune, R.J. Salawitch, A.E. Dessler, and J.G. Anderson, Balloon-borne *in situ* measurements of ClO and ozone: implications for heterogeneous chemistry and mid-latitude ozone loss, *Geophys. Res. Lett.*, 20, 1795-1708, 1993.
- Bell, W., G. Duxbury, and D.D. Stuart, High resolution spectra of v<sub>4</sub> band of chlorine nitrate, *J. Mol. Spectrosc.*, 152, 283-297, 1992.
- Boughner, R. J., J.C. Larson, and M. Natarajan, The influence of NO and ClO variations at twilight on the interpretation of solar occultation measurements, *Geophys. Res. Lett.*, 7, 231-234, 1980.
- Brown, L. R., M.R. Gunson, R.A. Toth, F.W. Irion, C. I'. Rinsland and A. Goldman, The 1995 atmospheric trace molecule spectroscopy experiment (ATMOS) line list, *Appl. Optics*, 35, 2828-2848, 1996.
- Cantrell, C. A., J.A. Davidson, A.H. McDaniel, R. E. Shetter, and J.G. Calvert, Infrared absorption cross-sections for N<sub>2</sub>O<sub>5</sub>, *Chem. Phys. Lett.*, 148, 358-362, 1988.
- Chance, K. *et al.*, Simultaneous measurements of stratospheric HO<sub>x</sub>, NO<sub>x</sub>, and Cl<sub>x</sub> - comparison with a photochemical model, *J. Geophys. Res.*, 101, 9031-9043, 1996.
- Chang, A.Y. *et al.*, A comparison of measurements from ATMOS and instruments aboard the ER-2 aircraft: halogenated gases, *Geophys. Res. Lett.*, 23, 2393-2396, 1996a.
- Chang, A.Y. *et al.*, A comparison of measurements from ATMOS and instruments aboard the ER-2 aircraft: tracers of atmospheric transport, *Geophys. Res. Lett.*, 25, 2393-2396, 1996b.
- Crutzen, P. J., The influence of nitrogen oxides on the atmospheric ozone content, *J. Roy. Met. Soc.*, 96, 320-325, 1970.
- DeMore, W. B. *et al.*, Chemical kinetics and photochemical data for use in stratospheric modeling, *JPL Publ. 94-26*, 1994.

- Dessler, A.E. *et al.*, Balloon-borne measurements of ClO, N(), and O<sub>3</sub> in a volcanic cloud - an analysis of heterogeneous chemistry between 20 and 30 km, *Geophys. Res. Lett.*, **20**, 2527-2530, 1993.
- Fahey, D.W. *et al.*, *In situ* measurements constraining the role of sulfate aerosols in mid-latitude ozone depletion, *Nature*, **363**, 509-514, 1993.
- Fahey, D.W. *et al.*, *In situ* measurements of total reactive nitrogen, total water, and aerosol in a polar stratospheric cloud in the Antarctic, *J. Geophys. Res.*, **94**, 11299-11315, 1989.
- Gao, R.S. *et al.*, Partitioning of the reactive nitrogen reservoir in the lower stratosphere of the southern hemisphere: observations and modeling, *J. Geophys. Res., submitted*, 1997.
- Gordley, L.L. *et al.*, validation of nitric oxide and nitrogen dioxide measurements made by Halogen occultation Experiment for UARS platform, *J. Geophys. Res.*, **101**, **10241-10266**, 1996.
- Hanson, 1). R., and A.R. Ravishankara, Heterogeneous chemistry of bromine species in sulfuric-acid under stratospheric conditions, *Geophys. Res. Lett.*, **22**, 385-388, 1995.
- Hanson, 1).1{ ... A.R. Ravishankara and E. It. Lovejoy, Reactions of BrONO<sub>2</sub> with H<sub>2</sub>O on submicron sulfuric acid aerosol and the implications for the lowest stratosphere, *J. Geophys. Res.*, **101**, 9063-9069, 1996.
- Jaeglé, L., Stratospheric chlorine and nitrogen chemistry: observations and modeling, Ph.D. Dissertation, 159 pp., California Institute of Technology, December 1995.
- Jaeglé, L. *et al.*, *In situ* measurements of NO<sub>x</sub>/NO ratio for testing atmospheric photochemical models, *Geophys. Res. Lett.*, **21**, 2555-2558, 1994.
- Johnston, H. S., Reduction in stratospheric ozone by nitrogen oxide catalysts from SST exhaust, *Science*, **173**, 517-522, 1971.
- Jucks, K. W. *et al.*, Ozone production and loss rate measurements in the middle stratosphere, *J. Geophys. Res.*, **101**, 28785-28792, 1996.
- Kawa, S. R., *et al.*, Interpretation of NO<sub>x</sub>/NO<sub>y</sub> observations from AASIE-II using a model of chemistry along trajectories, *Geophys. Res. Lett.*, **20**, 2507-2510, 1993.
- Keim, E.R. *et al.*, Measurements of the NO<sub>y</sub> - N<sub>2</sub>O correlations in the lower stratosphere: latitudinal and seasonal changes and model comparisons, *J. Geophys. Res., submitted*,

- 1997.
- Kinnison, 1).13., K.E. Grant, P.S. Connell, D.A. Rotman, and D.J. Wuebbles, The chemical and radiative effects of the Mount Pinatubo eruption, *J. Geophys. Res.*, 99, 25705-25731, 1994.
- Koike, M. *et al.*, Impact of Pinatubo aerosols on the partitioning between NO<sub>2</sub> and HNO<sub>3</sub>, *Geophys. Res. Lett.*, 21, 597-600, 1994.
- Kondo, Y., T. Sugita, R.J. Salawitch, M. Koike, and T. Deshler, The effect of Pinatubo aerosols on stratospheric NO, *J. Geophys. Res.*, 102, 1205-1213, 1997.
- Kondo, Y. et al., Diurnal variation of Iltic-oxide in the upper-stratosphere, *J. Geophys. Res.*, 95, 22513-22522, 1990.
- Lary D.J. *et al.*, carbon aerosols and atmospheric photochemistry, *J. Geophys. Res.*, *in press*, 1997.
- Loewenstein, M., J.R. Podolske, K.R. Chan, and S.E. Strahan, Nitrous oxide as a dynamical tracer in the 1987 Airborne Antarctic Ozone Experiment, *J. Geophys. Res.*, 94, 11589-11598, 1989.
- May, R.D., and R.R. Fried], Integrated band intensities of HO<sub>2</sub>NO<sub>2</sub> at 220K, *J. Quant. Spectrosc. Radiat. Transfer*, 52, 257-266, 1993.
- McCormick, M. P., L.W. Thomason, and C.R. Trepte, Atmospheric effects of the Mt. Pinatubo eruption, *Nature*, 373, 399-404, 1995.
- McElroy, C.T., C. Midwinter, D.V. Barton, and R.B. Hall, A comparison of J-values from the composition and photodissociative flux measurement with model-calculations, *Geophys. Res. Lett.*, 22, 1365-1368, 1995.
- McElroy, M. B., R.J. Salawitch and K. Minschwaner, The changing stratosphere, *Planet. Space Sci.*, 40, 373-401, 1992.
- Michelsen, H.A. *et al.*, Stratospheric chlorine partitioning: constraints from shuttle measurements of [HCl], [ClNO<sub>3</sub>], and [ClO], *Geophys. Res. Lett.*, 23, 2361-2364, 1996.
- Michelsen, H. A., R.J. Salawitch, P.O. Wennberg, and J.G. Anderson, Production of O(<sup>1</sup>D) from photolysis of O<sub>3</sub>, *Geophys. Res. Lett.*, 21, 2227-2230, 1994.
- Newchurch, M.J. *et al.*, Stratospheric NO and N02 abundances from ATMOS solar-occultation

- measurements, *Geophys. Res. Lett.*, 23, 2373-2376, 1996.
- Osterman, G. Il. *et al.*, Balloon-borne measurements of stratospheric radicals and their precursors: implications for production and loss of ozone, *Geophys. Res. Lett., in press*, 1997.
- Pickett, H. M., and D.B. Peterson, Comparison of measured stratospheric OH with prediction, *J. Geophys. Res.*, 101, 16789-16796, 1996.
- Pickett, H. M., and D.B. Peterson, Stratospheric OH measurements with a far-infrared limb observing spectrometer, *J. Geophys. Res.*, 98, 20507-205] 5, 1993.
- Plumb, R.A. and M.K.W. Ko, Interrelationships between mixing ratios of long-lived stratospheric Constituents, *J. Geophys. Res.*, 97, 1014 -10156, " 1992.
- Prather, M., Catastrophic loss of stratospheric ozone in dense volcanic clouds, *J. Geophys. Res.*, 97, 10187-10191, 1992.
- Ravishankara, A.R. and D.R. Hanson, Differences in the reactivity of type-1 polar stratospheric clouds depending on their phase, *J. Geophys. Res.*, 101, 3885-3890, 1996.
- Renard, J.-D. *et al.*, Vertical distribution of nighttime stratospheric NO<sub>2</sub> from balloon measurements: comparison with models, *Geophys. Res. Lett.*, 24, 73-76, 1997.
- Rinsland, C. P., *et al.*, ATMOS/ATLAS-2 measurements of stratospheric chlorine and reactive nitrogen partitioning inside and outside the November 1994 Antarctic vortex, *Geophys. Res. Lett.*, 23, 2365-2368, 1996.
- Rodriguez, J. M., M.K.W. Ko, N. I). Sze, C.W. Heisey, G.K. Yue, M. I'. McCormick, Ozone response to enhanced heterogeneous processing after the eruption of Mt-Pinatubo, *Geophys. Res. Lett.*, 21, 209-212, 1994.
- Roscoe, H .K., and J.A. Pyle, Measurements of solar occultation: the error in a naive retrieval if the constituent's concentration changes, *J. Atmos. Chem.*, 5, 323-341, 1987.
- Roscoe, H .K., J.R. Drummond, and R.F. Jar not, Infrared measurements of stratospheric composition, III, the daytime changes of NO and NO<sub>2</sub>, *Proc. r. Sot, London A*, 375 507-528, 1981.
- Russell, J.M. *et al.*, Measurements of odd nitrogen compounds in the stratosphere by the ATMOS experiment on Spacelab 3, *J. Geophys. Res.*, 93, 1718-1736, 1988.

- Salawitch, R.J. *et al.*, The distribution of hydrogen, nitrogen, and chlorine radicals in the lower stratosphere implications for changes in O<sub>3</sub> due to emission of NO<sub>y</sub> from supersonic aircraft, *Geophys. Res. Lett.*, 21, 2547-2550, 1994a.
- Salawitch, R.J. *et al.*, The diurnal variation of hydrogen, nitrogen, and chlorine radicals: implications for the heterogeneous production of HNO<sub>2</sub>, *Geophys. Res. Lett.*, 21, 2551-2554, 1994b.
- Sen, B., G.C. Toon, J.-F. Blavier, E.L. Fleming, and C. II. Jackman, Balloon-borne observations of mid-latitude fluorine abundance, *J. Geophys. Res.*, 101, 9045-9054, 1996.
- Solomon, S., R.W. Portmann, R.R. Garcia, L.W. Thomason, and M.P. McCormick, The role of aerosol variations in anthropogenic ozone depletion at northern midlatitudes, *J. Geophys. Res.*, 101, 6713-6727, 1996.
- Stachnik, R. A., J.C. Hardy, J.A. Tarsala, and J.W. Waters, Submillimeterwave heterodyne measurements of stratospheric ClO, HCl, O<sub>3</sub>, and HO<sub>2</sub>: first results, *Geophys. Res. Lett.*, 19, 1931-1934, 1992.
- Stimpfle, R.M. *et al.*, The response of ClO radical concentrations to variations in NO<sub>2</sub> radical concentrations in the 10WCI stratosphere, *Geophys. Res. Lett.*, 21, 2543-2546, 1994.
- Tie, X. X., G. Brasseur, The importance of heterogeneous bromine chemistry in the lower stratosphere, *Geophys. Res. Lett.*, 23, 2505-2508, 1996.
- Toon, G. C., The JPL MkIV interferometer, *Opt. Photonics News*, 2, 19-21, 1991.
- Webster, C. II. *et al.*, Evolution of HCl concentrations in the lower stratosphere from 1991 to 1996 following the eruption of Mt. Pinatubo, *Geophys. Res. Lett.*, submitted, 1997.
- Webster, C. R., R. L. May, M. Allen, I. Jaeglé, M.P. McCormick, Balloon profiles of stratospheric NO<sub>2</sub> and HNO<sub>3</sub> for testing the heterogeneous hydrolysis of N<sub>2</sub>O<sub>5</sub> on sulfate aerosols, *Geophys. Res. Lett.*, 21, 53-56, 1994.
- Webster, C.I{., R.D. May, R. Toumi, and J.A. Pyle, Active nitrogen partitioning and the nighttime formation of N<sub>2</sub>O<sub>5</sub> in the stratosphere - simultaneous *in situ* measurements of NO, NO<sub>2</sub>, HNO<sub>3</sub>, O<sub>3</sub>, and N<sub>2</sub>O using the BLISS diode-lascl spectrometer, *J. Geophys. Res.*, 95, 13851-13866, 1990.
- Wennberg, P.O. *et al.*, Removal of stratospheric O<sub>3</sub> by radicals *in situ* measurements of OH,

HO<sub>2</sub>, NO, N0<sub>2</sub>, C1O, and BrO, *Science*, 266, 398-404, 1994.

Yue, G.K., L.R. Poole, P.-H. Wang, and E.W. Chiou, Stratospheric aerosol acidity, density, and refractive index deduced from SAGA II and NMC temperature data, *J.Geophys. Res.*, 99, 3727-3738, 1994.

**Figure 1.** NO and NO<sub>2</sub> profiles at sunset of 25 September 1993 with and without diurnal corrections. Error bars have been displaced in altitude for visual clarity.

**Figure 2.** Ozone vmr profiles measured by *in situ* UV sensor during balloon ascent on 25 September 1993 and descent the following day. MkIV measurement of O<sub>3</sub> during sunset of 25 September from the same balloon gondola as the UV instrument is included for comparison between the two measurement techniques.

**Figure 3.** Observed (symbols) and calculated (lines) vmr profiles of NO<sub>y</sub> and member species, as indicated, measured at sunset by MkIV at 35° N on 25 September 1993. Sunrise profiles for N<sub>2</sub>O<sub>5</sub> are also shown. The NO<sub>y</sub> profile represents only the sum of measured nitrogen oxides.

**Figure 4.** Correlation of vmrs of NO<sub>y</sub> and N<sub>2</sub>O measured at sunset by MkIV (25 September 1993) and by instruments aboard the ER-2 aircraft, (14 February and 2, 4 November 1994. )

**Figure 5.** The midday, sunset and sunrise values for NO<sub>x</sub> and 2-N<sub>2</sub>O<sub>5</sub> are presented for the altitudes of 32, 26, and 22 km. The calculated values plotted illustrate the behavior of the model (sunset: red lines; sunrise: blue line) during the periods of MkIV measurement and the changes in NO<sub>x</sub> due to variations in albedo.

**Figure 6.** HALOE (triangles) and MkIV measurements at sunset of NO and NO<sub>2</sub> on 25 September 1993. The measurements have been displaced in altitude for visual clarity. The modeled profiles (solid line) of NO and NO<sub>2</sub> from a simulation constrained by MkIV measurements of precursors is included for comparison.

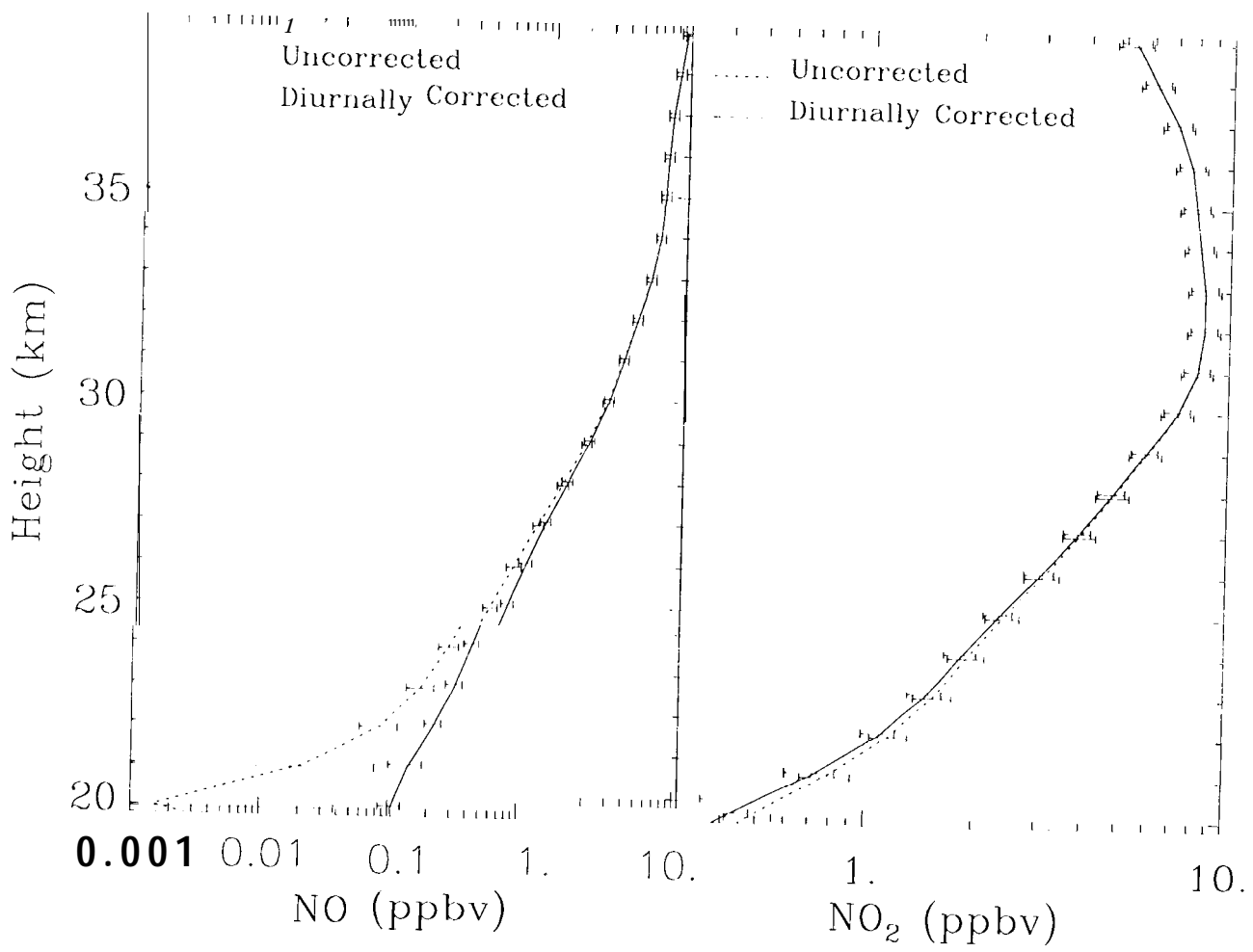
**Figure 7.** The fractional difference in measured and modeled NO<sub>2</sub> for September 1990, April 1993, September 1993, and May 1994 balloon flights of the MkIV. Model simulations are constrained by the MkIV measurements of precursors appropriate for each balloon flight.

**Figure 8.** Observed values of NO, NO<sub>2</sub>, and NO/NO<sub>2</sub> during sunrise, midday, and sunset during the September 1993 balloon flight. The model curves represent the same simulations illustrated in Figure 5.

**Figure 9.** Measured and recommended rates of the reaction  $\text{NO} + \text{O}_3 \rightarrow \text{NO}_2 + \text{O}_2$ . Recommended rate and its error is from JPL 94-26. Measurements are shown with their respective errors. References to individual measurements are listed in JPL 94-26.

**Figure 10.** The observed and calculated profiles of  $\text{NO}_x/\text{NO}_y$  as a function of altitude. Results from three balloon flights are shown for differing levels of aerosol surface area: pre Mt. Pinatubo eruption (Ft. Sumner, Sept. 1990) moderate recovery from the eruption (Ft. Sumner, Sept. 1993), highly perturbed loading (Daggett, Apr. 1993). Three simulations describe each balloon flight: (1) gas phase only (solid line), (2) gas phase and  $\text{N}_2\text{O}_5$  hydrolysis (dotted line), and (3) gas phase and all heterogeneous reactions (dashed line).

**Figure 11.** The observed and calculated profiles of  $\text{NO}_x/\text{NO}_y$  as a function of aerosol surface area. Note changes in both abscissa and ordinate scale in three panels. The model curves represent the same three simulations illustrated in Figure 10.



Ft. Sumner Balloon Flight 930925  
UV in situ and MarkIV Ozone

